Human kidney-derived hematopoietic stem cells can support long-term multilineage hematopoiesis

Steicy Sobrino, Chrystelle Abdo, Bénédicte Neven, Adeline Denis, Nathalie Gouge-Biebuyck, Emmanuel Clave, Soëli Charbonnier, Tifanie Blein, Camille Kergaravat, Marion Alcantara, et al.

Landmark Communications

Human kidney-derived HSPCs can support long-term multilineage hematopoiesis

Steicy Sobrino (1, 4), Chrystelle Abdo (2, 4), Bénédicte Neven (3, 4), Adeline Denis (1), Nathalie Gouge-Biebuyck (5), Emmanuel Clave (6), Soëli Charbonnier (1), Tifanie Blein (1), Camille Kergaravat (6), Marion Alcantara (2, 4), Patrick Villarese (2), Romain Berthaud (4, 5), Laurène Dehoux (5), Souha Albinni (7), Esma Karkeni (10), Chantal Lagresle-Peyrou (1), Marina Cavazzana (1, 4), Rémi Salomon (4, 5), Isabelle André (1), Antoine Toubert (4, 6), Vahid Asnafi (2, 4), Capucine Picard (1, 4, 8), Stéphane Blanche (3, 4), Elizabeth Macintyre (2, 4), Olivia Boyer (4, 5), Emmanuelle Six (1) #*, Julien Zuber (1, 4, 9) #*

1- INSERM UMR 1163, Institut IMAGINE, Paris, France

2- Laboratoire d'Onco-Hématologie, Hôpital Necker, Assistance-Publique Hôpitaux de Paris, Paris, France

3- Service d'Immuno-Hématologie pédiatrique, Hôpital Necker, Assistance-Publique Hôpitaux de Paris, Paris, France

4- Université Paris Cité, France

5- Service de Néphrologie Pédiatrique, Hôpital Necker, Assistance-Publique Hôpitaux de Paris, Paris, France

6- INSERM UMRS 1160, Institut de Recherche Saint Louis, Paris, France

7- Etablissement Français du Sang Ile-de-France, Hôpital Necker, Assistance-Publique Hôpitaux de Paris, Paris, France

8- CEDI, Hôpital Necker, Assistance-Publique Hôpitaux de Paris, Paris, France

9- Service des Maladies du Rein et Métabolisme, Transplantation et Immunologie Clinique, Hôpital Necker, Assistance-Publique Hôpitaux de Paris, Paris, France

10- Cytometry and Biomarkers UTechS, Center for Translational Science, Institut Pasteur, Paris, France.

# These senior authors contributed equally to the study.

***Corresponding authors:**

Dr. Emmanuelle Six, PhD, INSERM UMR_S1163, Imagine Institute. 24 Bd de Montparnasse 75015 Paris, France

Email: emmanuelle.six@inserm.fr

ORCID: 0000-0001-7806-0968

Prof. Julien Zuber, MD, PhD, INSERM UMR_S1163, Imagine Institute. 24 Bd de Montparnasse 75015 Paris, France

Email: julien.zuber@aphp.fr

Phone: 0033144495441, Fax: 0033144494230

Twitter handle : @julienzuber

ORCID: 0000-0001-6741-9330

Running title:

Human kidney-derived HSCs

Word count: Abstract: 144; Whole text: 1502

ABSTRACT

Long-term multilineage hematopoietic donor chimerism occurs sporadically in patients who receive a transplanted solid organ enriched in lymphoid tissues, such as the intestine or liver. Graft-versus-host (GvH)-reactive donor T cells were found to promote engraftment of graft-derived hematopoietic stem cells (HSCs) by making space in the bone marrow. We report here full (>99%) multilineage, donor-derived hematopoietic chimerism in a pediatric kidney transplant recipient with a syndromic combined immune deficiency, leading to transplant tolerance. There is currently no evidence for the presence of kidney-resident hematopoietic stem cells in any mammal species. We found, however, that human kidney-derived HSCs took up long-term residence in the recipient's bone marrow and gradually replaced their host counterparts leading to blood type conversion and to full donor chimerism in both lymphoid and myeloid lineages. These findings highlight the existence of human kidney-derived HSC with self-renewal ability able to support multilineage hematopoiesis.

KEYWORDS

Kidney allograft

Hematopoietic Stem and Progenitor Cells

Chimerism

INTRODUCTION

Schimke immune-osseous dysplasia (SIOD) is a rare autosomal recessive disorder caused by biallelic variants in the *SMARCAL1* gene (SWI/SNF2-related, matrix-associated, actin-dependent regulator of chromatin, subfamily a-like 1). SMARCAL1 plays a key role in maintaining DNA integrity, while its deficiency entails a systemic syndrome encompassing spondyloepiphyseal dysplasia, short stature, kidney failure, primary combined immune deficiency and accelerated arteriosclerosis [1,2]. SIOD-related renal impairment, resulting from podocyte dysfunction, includes different forms of focal segmental glomerulosclerosis that progress to end stage renal disease (ESRD) at an average age of 8.7 years [2]. The hallmark features of SIOD-associated combined immune deficiency include fluctuating lymphocyte counts below normal ranges, low thymic output, reduced naïve T cell compartments, defective IL-7Rα expression, as well as B- and NK-cell dysfunction [3].

HSCT (hematopoietic stem cell transplantation) represents the primary treatment for several severe forms of CID [4]. After conditioning, CD34+ hematopoietic stem and progenitor cells (HSPCs) are transplanted, and engraftment of the most immature hematopoietic stem cells (HSCs) in the bone marrow (BM) supports full immune reconstitution. HSCT, prior to or combined with kidney transplantation, may appear to be the ideal strategy in SIOD patients to tackle simultaneously ESRD and immune deficiency [5]. However, the outcomes of HSCT were reportedly very poor with SIOD [5], following conventional cytoreductive conditioning, being much lower than those usually observed in patients with common primary immunodeficiency syndromes [4]. In addition to the usual threats inherent to HSCT, the SIOD-related debilitated state (i.e. advanced or terminal renal failure, cerebrovascular events, increased sensitivity to genotoxic drugs) may account for the high mortality rate. In this respect, the recent report of 3 SIOD patients, in whom the sequential T-cell- and B-cell- depleted HSCT, after reduced

conditioning, and kidney transplant from the same donor, induced full hematopoietic chimerism and transplant tolerance, has the potential to be a game-changer [6].

However, before this recent study offered a new therapeutic avenue, isolated kidney transplantation had long been recognized as a suitable first-line therapeutic strategy, in the absence of profound T-cell defect. Here, we report a case of an SIOD patient who developed multilineage, sustained donor hematopoietic chimerism and transplant tolerance after an isolated kidney transplantation.

SHORT METHODS:

Hematopoietic chimerism:

Monoclonal HLA class I allele-specific antibodies were used to discriminate HLA-A23+ (clone BIH0964) donor and HLA-A2+ (clone FH0037, One Lambda, Canoga Park, CA) recipient cells, in combination with pan-HLA class I antibodies, as previously reported [7,8]. Donor's and recipient's HLA types are shown in Table S1. Donor (KMR045)- and recipient (KMR047)-specific single nucleotide polymorphisms (SNPs) were also quantified in blood and bone marrow cells using quantitative polymerase chain reaction (KMRtype® and KMRtrack® chimerism monitoring reagents, GenDx, Utrecht, Netherlands).

sTREC measurement:

sjTRECs were quantified as described previously (online supplemental methods) [9].

HSPC phenotyping:

Patient hematopoietic stem and progenitor cells (HSPCs) were characterized from a 10-color multilabeled panel using the antibody described in online supplemental methods. Staining was

analyzed on a spectral flow analyzer (Sony SP6800) and the gating strategy presented in Figure2A.

Cytokine measurement:

Cytokine levels were measured from bone marrow supernatant, and the acquisitions were performed through SIMOA technology on Sp-X (Quanterix) for IFN-γ, IL-12p70, IL-1β, IL-4, IL-5, IL-6, IL-8, IL-22, TNF-α and IL-10 and on HD-X (Quanterix) for IL-18, respectively.

TCR beta sequencing and repertoire analysis:

TCR repertoire analysis were performed as described previously (online supplemental method)[10].

Ethical considerations:

The investigations and tailored therapies undertaken in the patient were approved by the local Institutional Review Board (CENEM 2018-OB, 05/05/2018) and consented by the legal representatives (parents) after written information.

RESULTS

Multilineage donor hematopoietic chimerism following kidney transplantation

The patient was a 3-year-old boy with SIOD who progressed to end-stage renal disease and received a first kidney transplant from a 25-year-old male, HLA-mismatched, deceased donor three months later (Figure S1). His immunosuppressive regimen included basiliximab induction therapy, and then tacrolimus, azathioprine and steroids. Epstein-Barr virus and cytomegalovirus serostatuses were both donor-positive and recipient-negative. Hence, he was given two pulses (375 mg/m^2) of rituximab and daily valganciclovir as prophylaxis against Epstein-Barr virus-driven posttransplant lymphoproliferative disorder and cytomegalovirus infection, respectively.

Landmark Communications

In the context of combined immune deficiency, the persistence of profound T-cell lymphopenia led to azathioprine, prednisone and tacrolimus withdrawal at post-operative day (POD) 20, 31 and 81, respectively (Figure S1). At 3 months post-transplant, within the week following complete immunosuppressive drug withdrawal, he developed a febrile acute grade III GVHD, with skin rash, diarrhea and elevated levels of liver enzymes (Figure S1), concurrent with high donor chimerism among circulating T cells. Steroids and tacrolimus therapies were resumed on POD94 and POD104, respectively. High-dose steroids resulted in fever clearance and the resolution of skin lesions. However, the cholestasis and cytopenia worsened upon steroids, prompting initiation of an innovative cell-free donor-specific plasma therapy that successfully obtained the remission of acute GVHD, as previously reported [7]. As he recovered from GVHD-induced aplasia [7], his blood cell counts sharply increased and were maintained within normal ranges thereafter (Figure S2). Donor chimerism remained highly prominent among circulating T cells following GVHD remission (Figure 1A-B). More surprisingly, full chimerism was observed in all lymphoid and myeloid blood cell lineages (Figures 1A-C) and confirmed by molecular biology in total blood (Figure 1D). Additionally, the Rhesus C red blood cell antigen type changed to the donor type between POD131 and POD219 (Figure 1E). Given the tolerogenic state of full donor chimerism, immunosuppression was progressively tapered down. However, mild cholestasis and biopsy-proven chronic GVHD of the liver (POD361) led to the increase of steroid and tacrolimus dosing (Figures S1 and S2). Tacrolimus was definitively withdrawn at POD576 after a kidney graft biopsy had unveiled histologic features of calcineurin inhibitor-related nephrotoxicity (Figures S1 and S2). Importantly, the graft biopsy performed at POD501 was free of rejection (Figure S1). Steroids were definitively stopped at POD761, but the persistence of mild histological features of liver GVHD (POD740) required to continue azathioprine until POD864. The 3-year glomerular filtration rate was measured at 76

ml/mn/1.73m^2. At last follow-up (POD1542), the creatinine level was 0.33 mg/dL, while no protein was detected in the urine.

Donor-derived T and B-cell ontogeny

We next questioned whether immune reconstitution was associated with the emergence of donor-derived naïve T and B cells. At POD143, CCR7+ CD45RA+ naïve T cells were barely identified among the circulating donor T cells (Figure 1F), in keeping with the recirculation of alloreactive graft-derived memory T cells. However, the T-cell phenotype changed afterward, with an increasing frequency of naïve T cells of donor origin (Figure 1F, supplemental Table S2). Notably, sjTRECs (signal joint T-cell receptor excision circles) were not detected in the early posttransplant course, yet reached levels comparable to those of healthy donors at POD912 (Figure 1G). This indicates the appearance of recent thymic emigrants [11]. Similarly, as the patient recovered from B-cell lymphopenia (POD311), transitional (CD19+CD24++CD38++) circulating B cells (Figure 1H) were all of donor origin (Figure 1B). Subsequent emergence of CD27+ IgD- memory B cells, along with normal IgM, IgA and IgG levels, further established the recovery of immune functions (Figure 1H, Table S2). The patient completed his full vaccination schedule (Figure S1). Subsequent functional assays established immune responses to vaccines, including tetanus toxin-specific T cell proliferation, as well as anti-HBs, anti-VZV, and anti-pertussis toxin antibodies (Figure S1). Overall, these findings strongly suggested that donor-derived HSPCs were able to support hematopoiesis and immune reconstitution in the recipient.

Long-term residence of kidney-derived HSPCs in the recipient's bone marrow

Bone marrow (BM) aspiration was performed at POD156 because of persistent thrombocytopenia. We seized the opportunity to examine the presence of kidney-derived HSCs

contributing to full hematopoiesis reconstitution. Magnetically sorted CD34+ cells were phenotyped to fully characterize the different HSPC subpopulations (Figure 2A). Donor chimerism was measured at approximately 96% in BM CD34+ HSPCs by both quantitative PCR and flow cytometry (Figure 2B). Donor chimerism, however, varied greatly throughout the hematopoietic differentiation hierarchy (Figures 2A-B). Importantly, host-derived cells still accounted for 72% of the most immature HSCs. However, the host-derived cell contribution dropped to 42% in the downstream multipotent progenitors (MPPs) and far less among the more committed progenitors (Figure 2B). One year later, HSPCs of recipient origin were barely detected, except in the MPPs (Figure 2C).

We inferred that kidney-derived HSCs, with multilineage differentiation potential and self-renewal capacities, had taken up long-term residence in the recipient's BM.

Shift from narrowed to broad donor-derived T-cell repertoire

A recent report in intestinal transplant recipients showed that the presence of GvH-reactive T-cell clones in the BM correlated with the engraftment of donor CD34+ HSPCs and sustained mixed chimerism [12]. To address this latter hypothesis, we next investigated the repertoire distribution and diversity of circulating T cells. We studied TCRVβ repertoires at early (POD156/165) and late (POD521) time points, when the donor cell frequency was greater than 96 and 99%, respectively. Notably, in the early posttransplant course, the TCRβ VDJ repertoire was characterized by a few dominant clones detected in both the blood and BM (Figure 3A). Two clones, sharing the same V11-3 and J1-1 alleles, had a cumulative frequency greater than 70%. Given the low frequency of recipient-derived T cells, as evidenced by flow cytometry analysis, we inferred that these dominant clones were of donor origin. They accounted for a large repertoire overlap (more than 80%) between blood and BM compartments (in gray, Figure 3B). This highly skewed TCR repertoire was consistent with an antigen-driven expansion of T

cells. The accumulation of these few clones, associated with increased levels of inflammatory cytokines (IL-18 and IFN-γ) in the bone marrow, targeted by GVHD, strongly suggested than these clones had reactivity against host antigens (Figure 3C). Notably, bone marrow IL-18 and IFN-γ levels declined on POD521, in sharp contrast with the increased level of the immunoregulatory cytokine IL-10 (Figure S3), meanwhile circulating graft-derived clones were much less prominent (Figures 3C and 3D). As a fact, one year later, the clonal size distribution had become far more homogeneous (Figure 3D). We observed the emergence of 1598 new individualized clonotypes (Figure 3E) and increased Shannon diversity (Figure 3F) of the circulating TCRβ repertoire compared with one year earlier. Growing thymic output progressively diversified the T-cell repertoire.

DISCUSSION

The intestine contains a high burden of donor lymphoid tissues. Therefore, hematopoietic chimerism and GVHD are reportedly at higher rates after intestinal transplantation than after any other organ transplantations [8,13,14]. In contrast, GVHD has rarely been reported after kidney transplantation [15,16]. Kidney-resident T cells are supposedly far outnumbered by the numerous recipient T cells. However, in SIOD patients, immune cells are not only present in low numbers but are also overly sensitive to immunosuppressive drugs, especially genotoxic agents that damage DNA [5]. Hence, the immunosuppressive regimen, including a drug interfering with purine synthesis, like azathioprine or mycophenolate mofetil, may tip the balance toward donor T cells after transplantation by further impairing the proliferation of SIOD immune cells.

Sustained mixed chimerism can spontaneously occur after liver [17], intestinal and multivisceral [8,12,18] transplantation, resulting from the ability of donor HSPCs originating from hematopoietic tissues present in the transplanted organ to repopulate recipient bone marrow [18]. There is however no evidence for the presence of kidney-resident hematopoietic stem cells in any

mammal species, unlike in teleost fish [19]. To our knowledge, the present case is the first evidence that a human kidney contains enough HSCs to support long-term and multilineage hematopoiesis. The extensive blood washout during organ procurement does not support the intravascular origin of donor-derived CD34+ HSCs. Instead, it suggests the presence of kidney HSCs able to recirculate after transplantation. Notably, cells expressing hallmark primitive HSC markers were recently identified through single-cell transcriptomic analysis in human fetal kidneys from two individuals [20]. Furthermore, extramedullary HSPC reservoirs are increasingly recognized and well-characterized in humans [18,21]. Whether HSCs reside in specific niches or transiently pass through renal parenchyma has yet to be determined. Importantly, ischemic/hypoxic preconditioning was found to enhance the mobilization and recruitment of bone marrow HSC into peripheral ischemic tissues [22]. In the present case, ischemic stress might have occurred in the donor before organ procurement leading to the accumulation of HSCs in the kidneys. We cannot firmly exclude either that HSCs could have egressed from extra-renal lymphopoietic tissue, implanted along with the kidney, such as hilar lymph nodes. Overall, this breakthrough finding warrants further investigation to identify the phenotype, origin, frequency and localization of kidney-derived HSCs.

Spontaneous achievement of a full donor hematopoietic chimerism allowed complete discontinuation of immunosuppressive drugs. In the present case, cautious and slow drug tapering was more dictated by the persistence of mild GVHD symptoms than by the risk of graft rejection. Several protocols have successfully obtained mixed-chimerism-based transplant tolerance through combined kidney and hematopoietic cell transplantation [6,23,24]. Notably, in non-immunodeficient recipients, full donor chimerism was successfully obtained across HLA barrier, despite the use of nonablative conditioning regimen, by exploiting the ability of graft-vs-host reactive T cells to support donor HSCs engraftment [12,23]. The present case extends this concept by showing that graft-derived donor T cells can spontaneously promote hematopoietic

chimerism after an isolated kidney transplantation, at least in a young SIOD patient. However, this therapeutic approach takes a significant toll, as it may expose patients to life-threatening GVHD [23]. In this respect, the recent report from Bertaina and coll. is groundbreaking [6,24]. The use of αβ T-cell- and CD19+ B cell-depleted HSCT, following a reduced-intensity conditioning, was able to induce GVHD-free full chimerism in 3 SIOD recipients, resulting in transplant tolerance to a subsequent kidney allograft from the same haploidentical donor [6]. The optimal timing of such promising strategy has yet to be determined. In order to avoid the occurrence of aplasia in children under dialysis, whose management raises significant challenges, the sequential transplantation could be started ahead of dialysis onset.

Furthermore, our case demonstrates that a limited number of donor HSCs, supposedly very low within a kidney allograft, can readily outcompete their host counterparts in SIOD patients.

Disclosure statement:

J.Z. is inventor on the patent that describes the use of donor-specific plasmatherapy in patients with GVHD after HLA-mismatched transplantations.

Acknowledgments:

This work was supported by funding from the Emmanuel Boussard and Day Solvay Foundations and the Agence Nationale de la Recherche (ANR-10-IAHU-01 "Investissements d'Avenir" program; ANR-20-CE18-0004). We are grateful to Milena Hasan (Institut Pasteur) for critical advice on cytokine analysis.

Figure Legends:

Figure 1: Sustained and high levels of multilineage donor chimerism in blood

A) Flow cytometry contour plot showing a high level of donor T-cell and monocyte chimerism persisting after GVHD remission (POD 171). **B**) Percentage of donor chimerism over time, in lymphoid cell populations, including B cells (CD19+ CD3-), NK cells (CD56+ CD3-) and T cells (CD3+). **C**) Assessment of donor chimerism in the myeloid cell populations through flow cytometry. Blood cell subsets were defined as follows: platelets (CD41a+), monocytes (CD11b+ CD14+ CD15- CD3-), and neutrophils (CD11b+ CD14- CD15+ CD3-). **D**) Assessment of donor chimerism in whole blood through quantitative polymerase chain reaction. **E**) Graduate conversion from 100% recipient (O Rh D+ **C+** E- c+ e+ K-) to 100% donor (O Rh D+ **C-** E- c+ e+ K-) blood type. **F**) Flow cytometry contour plot showing the change in the frequency of naïve and memory T-cell subsets over time, according to their donor/recipient origin. **G**) Molecular measurement of sjTRECs demonstrating the growing thymic output post-transplant, compared to age-matched HDs (n=20). **H**) Flow cytometry contour plot showing the change in the frequency of transitional (CD38++ CD24++), naïve (IgD+ CD27-) and memory (CD27+) B-cell subsets over time.

Abbreviations: D, donor; POD, Postoperative day; R, recipient; HD, healthy donor.

Figure 2: Sustained and high levels of donor chimerism in the bone marrow hematopoietic progenitor subsets

A) Gating strategy used to study donor chimerism in different bone marrow-resident hematopoietic progenitors using flow cytometry. Flow cytometry contour plot showing the frequency of donor cells in each progenitor subset at POD156. HSPCs were gated on CD34+Lin- and defined as follows: CMP (CD38+ CD10- CD123dim CD45RA-), DCP (CD38+ CD10- CD45RA+ CD23+), HSC (CD133+ CD38- CD90+ CD45RA-), MPP (CD133+

CD38- CD90- CD45RA-), MLP (CD133+ CD38- CD90- CD45RA+), BNKP (CD38+ CD10+), GMP (CD38+ CD10-, CD45RA+ CD123+), and MEP (CD38+ CD10- CD45RA- CD123-). **B-C**) Assessment of donor chimerism in bone marrow lineage-negative CD34+ progenitors through molecular biology and flow cytometry at POD156 (**B**) and POD521 (**C**). The hierarchical organization of hematopoiesis is represented by a handful of lineage-negative CD34+ progenitors along a branched differentiation pathway.

Abbreviations: BNKP, B and NK progenitors; BM, bone marrow; DCP, dendritic cell progenitors; CMP, common myeloid progenitor; D, donor; ETP, early thymic progenitors; FACS, fluorescence-activated single cell sorting; GMP, granulocyte-monocyte progenitors; HSC, hematopoietic stem cell; MEP, megakaryocyte-erythroid progenitor; MLP, multipotent lymphoid progenitor; MPP, multipotent progenitor; POD, postoperative day; QPCR, quantitative polymerase chain reaction; R, recipient.

Figure 3: Shift from narrowed to broad donor-derived T-cell repertoire

A) Circos plots showing the diversity of Vβ and Jβ gene pairing in blood and bone marrow cells collected at POD165 and POD156, respectively. **B**) Cumulative abundance of the clonotypes identified either in the blood only, in the bone marrow only or in both (overlapping clones). The absolute number of clonotypes in each category is indicated. (n) **C**) IL-18 and IFN-γ cytokine quantification in BM plasma at POD156 and POD521 compared to HD BM plasma (n=3). **D**) Circos plots showing the diversity of Vβ and Jβ gene pairing in blood cells collected at POD521. **E**) Cumulative abundance of the circulating clonotypes identified either at POD165 only, at POD521 only or in both (overlapping clones). The absolute number of clonotypes in each category is indicated (n). **F**) The Shannon entropy index quantifies the amount of information in a variable; the greater the index is, the more diverse the TCR repertoire.

Figure S1: Clinical features and investigations undertaken during the post-transplant course

A 3-year-old SIOD patient underwent a first HLA-mismatched kidney transplantation from a 25-year-old male deceased donor, 84 days after dialysis onset. The persistence of a profound lymphopenia in the early post-transplant course led to azathioprine (Aza.), prednisone (Pred.), and then tacrolimus (Tac.) withdrawal at POD20, 31 and 81, respectively. Rash, fever, diarrhea and increased liver enzymes occurred within a week following tacrolimus discontinuation. The finding of concurrent high donor chimerism in peripheral blood led to the diagnosis of graft-vs-host disease (GVHD). The partial response to high-dose steroids prompted a rescue therapy, based on the administration of donor-specific antibody (DSA)-rich plasma, that dramatically improved liver, intestinal and bone marrow failures. Yet, a moderate increase in liver enzymes at one-year post-transplant suggested the persistence of a mild form of liver GVHD that was confirmed by biopsy on POD361. Interestingly, liver and intestinal biopsies were undertaken at POD740 as a screening for subclinical GVHD. The former still disclosed a mild inflammation, despite normal liver enzyme levels, while the latter was unremarkable.

Although DSA were readily detected in patient's serum following plasma infusion, subsequent testing for DSA at POD221 and POD1038 was negative. The patient underwent two kidney allograft biopsies at POD38 and POD501 that firmly ruled out rejection. However, the latest biopsy showed extensive interstitial fibrosis suggesting tacrolimus-related nephrotoxicity. The bone marrow aspirations that were performed at POD156, because of persistent thrombocytopenia, and later on at POD521, showed reduced megakaryocytes and normal cellularity, respectively. Following immune reconstitution, he had a complete vaccine schedule, each shot being indicated by a triangle. Functional assays demonstrated T-cell responses against pp65 CMV antigen and tetanus toxin, while he acquired serological responses against HBs,

Varicella Zoster virus, and pertussis vaccines. Administration of immunosuppressive drugs is indicated with colored bars. Red and brown arrows indicate rituximab pulses and DSA-rich plasma infusions, respectively.

Abbreviations: Ab, antibody; Aza., azathioprine; DSA, donor-specific antibody; GVHD, graft-vs-host disease; Haem. B, Haemophilus B; HBs, hepatitis B antigen; IBx, intestinal biopsy; LBx, liver biopsy; POD, post-operative day; Pred., prednisone; Tac., tacrolimus; TT, tetanus toxin; VZV, varicella zoster virus.

Figure S2: Laboratory features and immunosuppressive drug dosing during the post-transplant course

Abbreviations: Bx, biopsy.

Figure S3: Cytokine levels in bone marrow plasma

IL-12p70, IL-1β, IL-4, IL-5, IL-6, IL-8, IL-22, TNF-α and IL-10 cytokine quantification in BM plasma at POD156 and POD521 compared to HD BM plasma (n=3).

Table S1: Donor's and recipient's HLA types.

Table S2: Immune reconstitution after kidney transplantation.

Reference (or normal) ranges, which are the sets of values within which 95% of measurements from apparently healthy controls lie, are indicated within brackets. Patient's values outside the normal ranges are shown in red fonts.

References:

1. Boerkoel CF, Geary DF, O'Neill S, et al. Manifestations and treatment of Schimke immuno-osseous dysplasia: 14 new cases and a review of the literature. *Eur J Pediatr*. 2000;159(1-2):1-7. doi:10.1007/S004310050001
2. Lipska-Ziętkiewicz BS, Gellermann J, Boyer O, et al. Low renal but high extrarenal phenotype variability in Schimke immuno-osseous dysplasia. *PLOS ONE*. 2017;12(8):e0180926. doi:10.1371/JOURNAL.PONE.0180926
3. Bertulli C, Marzollo A, Doria M, et al. Expanding Phenotype of Schimke Immuno-Osseous Dysplasia: Congenital Anomalies of the Kidneys and of the Urinary Tract and Alteration of NK Cells. *Int J Mol Sci*. 2020;21(22):1-17. doi:10.3390/IJMS21228604
4. Neven B, Ferrua F. Hematopoietic Stem Cell Transplantation for Combined Immunodeficiencies, on Behalf of IEWP-EBMT. *Front Pediatr*. 2020;7. doi:10.3389/FPED.2019.00552
5. Baradaran-Heravi A, Lange J, Asakura Y, Cochat P, Massella L, Boerkoel CF. Bone marrow transplantation in Schimke immuno-osseous dysplasia. *Am J Med Genet A*. 2013;161A(10):2609-2613. doi:10.1002/AJMG.A.36111
6. Bertaina A, Grimm PC, Weinberg K, et al. Sequential Stem Cell-Kidney Transplantation in Schimke Immuno-osseous Dysplasia. *N Engl J Med*. 2022;386(24):2295-2302. doi:10.1056/NEJMOA2117028
7. Zuber J, Boyer O, Neven B, et al. Donor-targeted serotherapy as a rescue therapy for steroid-resistant acute GVHD after HLA-mismatched kidney transplantation. *Am J Transplant*. 2020;20(8):2243-2253. doi:10.1111/AJT.15827
8. Zuber J, Rosen S, Shonts B, et al. Macrochimerism in Intestinal Transplantation: Association With Lower Rejection Rates and Multivisceral Transplants, Without GVHD. *Am J Transplant*. 2015;15(10):2691-2703. doi:10.1111/AJT.13325
9. Clave E, Araujo IL, Alanio C, et al. Human thymopoiesis is influenced by a common genetic variant within the TCRA-TCRD locus. *Sci Transl Med*. 2018;10(457). doi:10.1126/SCITRANSLMED.AAO2966
10. Magnani A, Semeraro M, Adam F, et al. Long-term safety and efficacy of lentiviral hematopoietic stem/progenitor cell gene therapy for Wiskott-Aldrich syndrome. *Nat Med*. 2022;28(1):71-80. doi:10.1038/S41591-021-01641-X
11. Gaballa A, Clave E, Uhlin M, Toubert A, Arruda LCM. Evaluating Thymic Function After Human Hematopoietic Stem Cell Transplantation in the Personalized Medicine Era. *Front Immunol*. 2020;11. doi:10.3389/FIMMU.2020.01341
12. Fu J, Zuber J, Shonts B, et al. Lymphohematopoietic graft-versus-host responses promote mixed chimerism in patients receiving intestinal transplantation. *J Clin Invest*. 2021;131(8). doi:10.1172/JCI141698
13. Wu KH, Chan CK, Tsai C, et al. Effective treatment of severe steroid-resistant acute graft-versus-host disease with umbilical cord-derived mesenchymal stem cells. *Transplantation*. 2011;91(12):1412-1416. doi:10.1097/TP.0B013E31821ABA18
14. Grant D, Abu-Elmagd K, Mazariegos G, et al. Intestinal transplant registry report: global activity and trends. *Am J Transplant*. 2015;15(1):210-219. doi:10.1111/AJT.12979
15. Zacharias N, Gallichio MH, Conti DJ. Graft-versus-Host Disease after Living-Unrelated Kidney Transplantation. *Case Rep Transplant*. 2014;2014:1-3. doi:10.1155/2014/971426

16. Guo Y, Ding S, Guo H, et al. Graft-versus-host-disease after kidney transplantation: A case report and literature review. *Medicine*. 2017;96(26). doi:10.1097/MD.0000000000007333
17. Alexander SI, Smith N, Hu M, et al. Chimerism and tolerance in a recipient of a deceased-donor liver transplant. *N Engl J Med*. 2008;358(4):369-374. doi:10.1056/NEJMOA0707255
18. Fu J, Zuber J, Martinez M, et al. Human Intestinal Allografts Contain Functional Hematopoietic Stem and Progenitor Cells that Are Maintained by a Circulating Pool. *Cell Stem Cell*. 2019;24(2):227-239.e8. doi:10.1016/J.STEM.2018.11.007
19. Paik EJ, Zon LI. Hematopoietic development in the zebrafish. *International Journal of Developmental Biology*. 2010;54(6-7):1127-1137.
20. Hwang JW, Desterke C, Loisel-Duwattez J, Griscelli F, Bennaceur-Griscelli A, Turhan AG. Detection of Hematopoietic Stem Cell Transcriptome in Human Fetal Kidneys and Kidney Organoids Derived From Human Induced Pluripotent Stem Cells. *Front Cell Dev Biol*. 2021;9:668833. doi:10.3389/fcell.2021.668833
21. Mende N, Bastos HP, Santoro A, et al. Unique molecular and functional features of extramedullary hematopoietic stem and progenitor cell reservoirs in humans. *Blood*. 2022;139(23):3387-3401. doi:10.1182/BLOOD.2021013450
22. de Falco E, Porcelli D, Torella AR, et al. SDF-1 involvement in endothelial phenotype and ischemia-induced recruitment of bone marrow progenitor cells. *Blood*. 2004;104(12):3472-3482. doi:10.1182/BLOOD-2003-12-4423
23. Zuber J, Sykes M. Mechanisms of Mixed Chimerism-Based Transplant Tolerance. *Trends Immunol*. 2017;38(11):829-843. doi:10.1016/J.IT.2017.07.008
24. Spitzer TR, Sachs DH. Transplantation Tolerance through Hematopoietic Chimerism. *N Engl J Med*. 2022;386(24):2332-2333. doi:10.1056/NEJME2204651

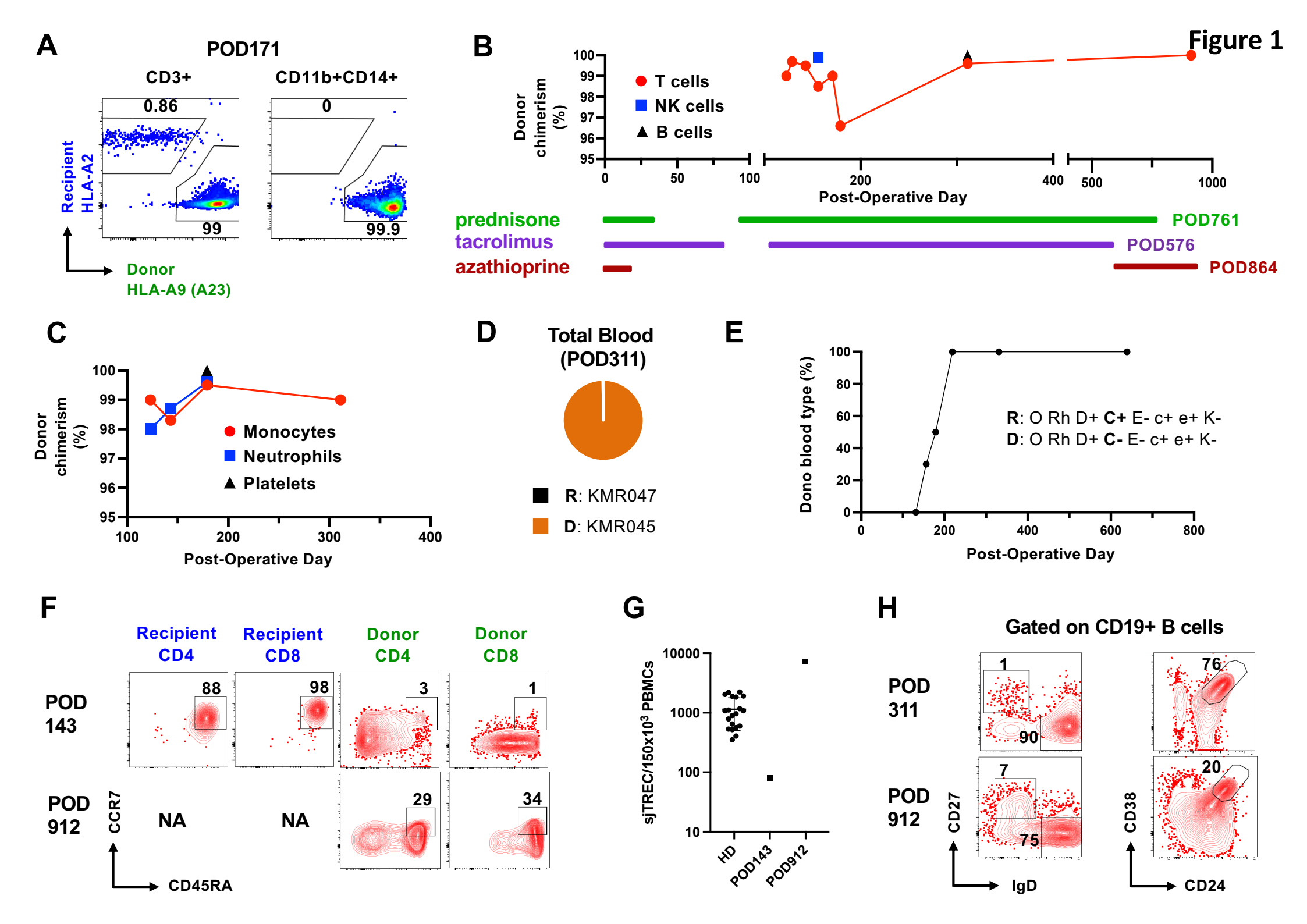
Figure 1
A
POD171
CD3+
CD11b+CD14+
0.86
0
99
99.9
Recipient HLA-A2
Donor HLA-A9 (A23)
B
Donor chimerism (%)
T cells
NK cells
B cells
Post-Operative Day
prednisone
tacrolimus
azathioprine
POD761
POD576
POD864
C
Donor chimerism (%)
Monocytes
Neutrophils
Platelets
Post-Operative Day
D
Total Blood (POD311)
R: KMR047
D: KMR045
E
Dono blood type (%)
R: O Rh D+ C+ E- c+ e+ K-
D: O Rh D+ C- E- c+ e+ K-
Post-Operative Day
F
Recipient CD4
Recipient CD8
Donor CD4
Donor CD8
POD 143
POD 912
88
98
3
1
29
34
NA
NA
CCR7
CD45RA
G
sjTREC/150x10³ PBMCs
HD
POD143
POD912
H
Gated on CD19+ B cells
POD 311
POD 912
1
90
7
75
76
20
CD27
IgD
CD38
CD24

Figure 2

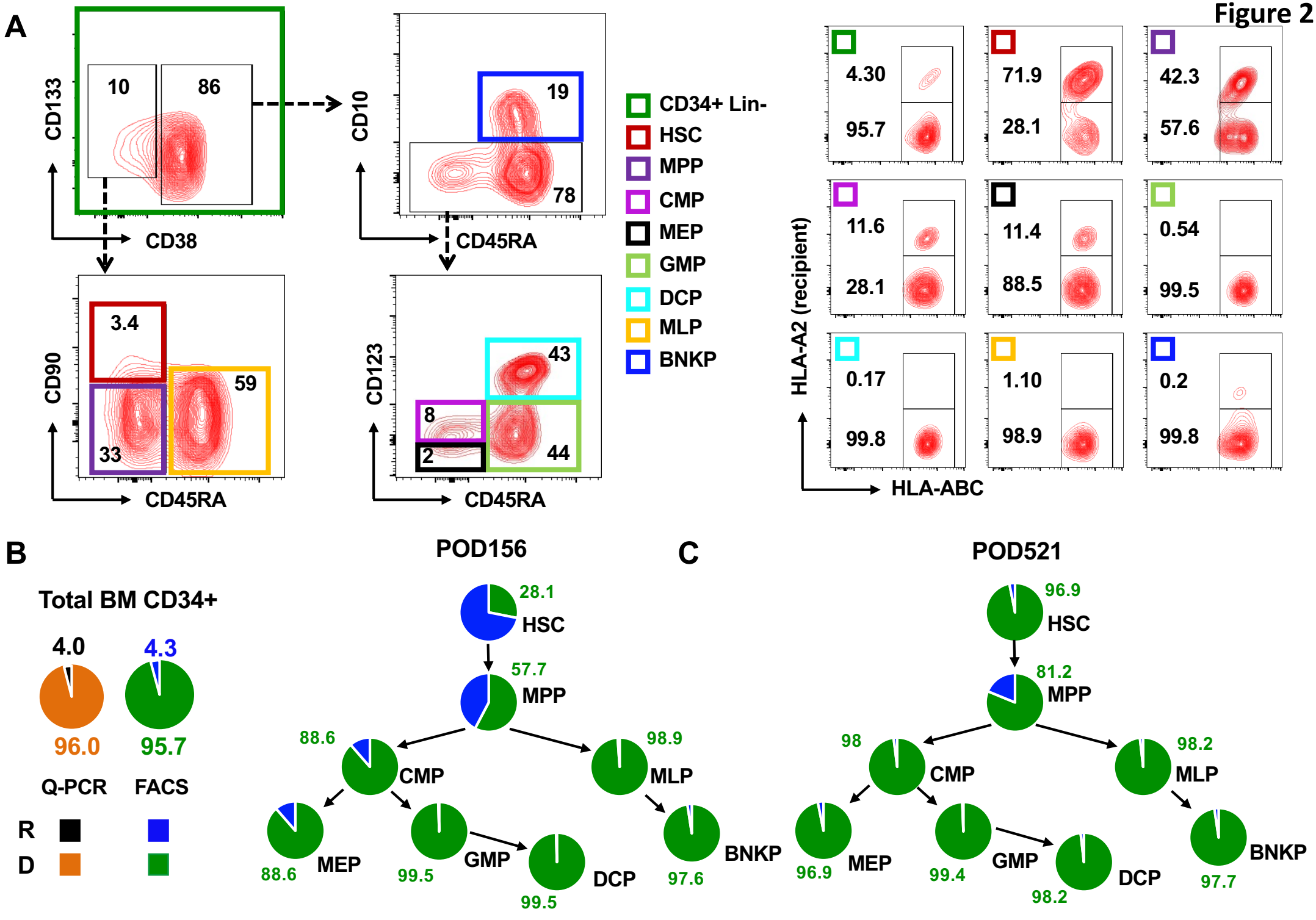
A
CD133
10
86
CD38
CD10
19
78
CD45RA
CD90
3.4
59
33
CD45RA
CD123
43
8
44
2
CD45RA
CD34+ Lin-
HSC
MPP
CMP
MEP
GMP
DCP
MLP
BNKP
4.30
95.7
71.9
28.1
42.3
57.6
11.6
28.1
11.4
88.5
0.54
99.5
0.17
99.8
1.10
98.9
0.2
99.8
HLA-A2 (recipient)
HLA-ABC
B
Total BM CD34+
4.0
4.3
96.0
95.7
Q-PCR
FACS
R
D
POD156
28.1
HSC
57.7
MPP
88.6
CMP
98.9
MLP
88.6
MEP
99.5
GMP
99.5
DCP
97.6
BNKP
C
POD521
96.9
HSC
81.2
MPP
98
CMP
98.2
MLP
96.9
MEP
99.4
GMP
98.2
DCP
97.7
BNKP

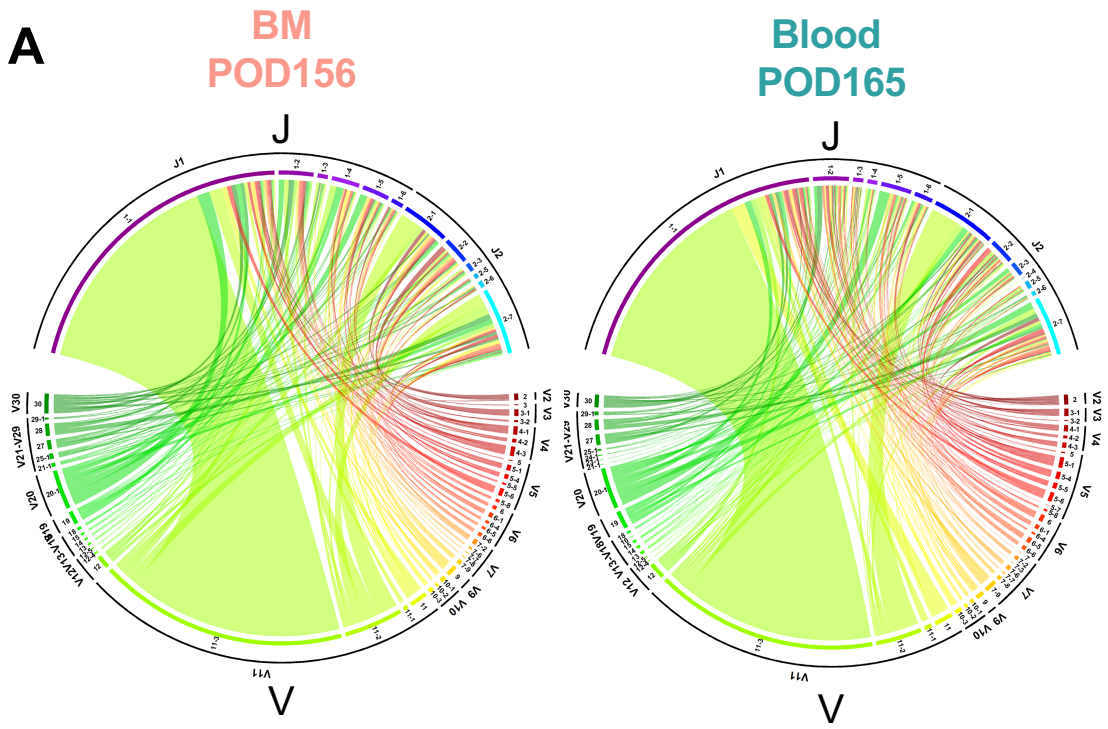
A
BM
POD156
Blood
POD165
J
V

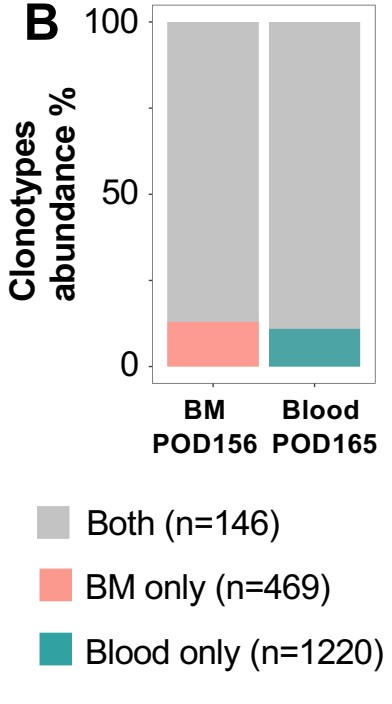
B
Clonotypes abundance %
100
50
0
BM POD156
Blood POD165
Both (n=146)
BM only (n=469)
Blood only (n=1220)

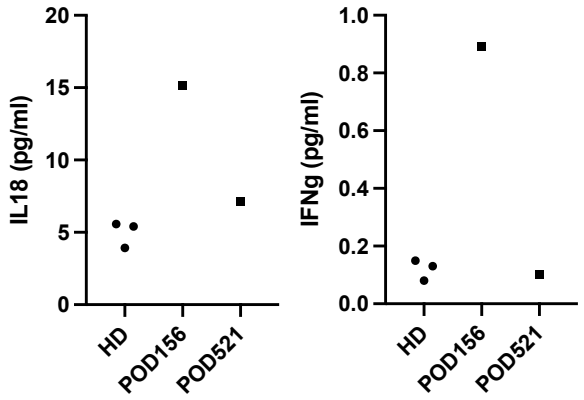
C
BM Plasma
IL18 (pg/ml)
IFNg (pg/ml)
HD
POD156
POD521

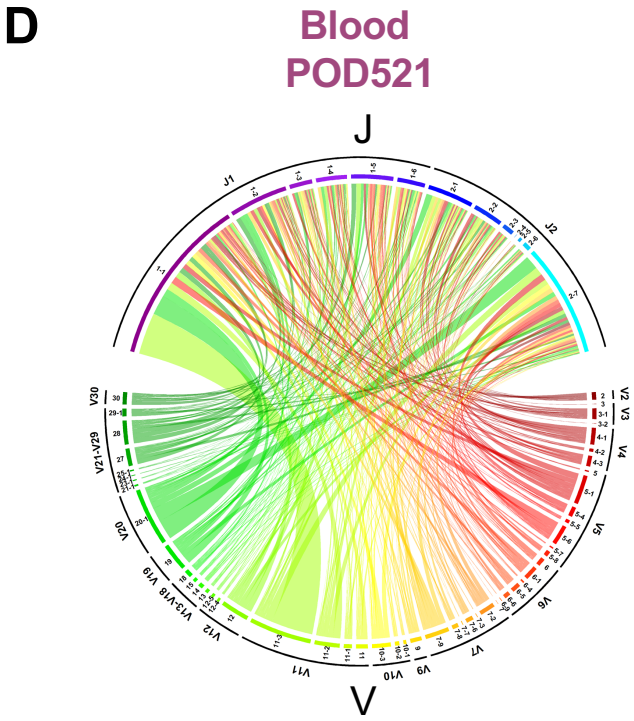
D
Blood
POD521
J
V

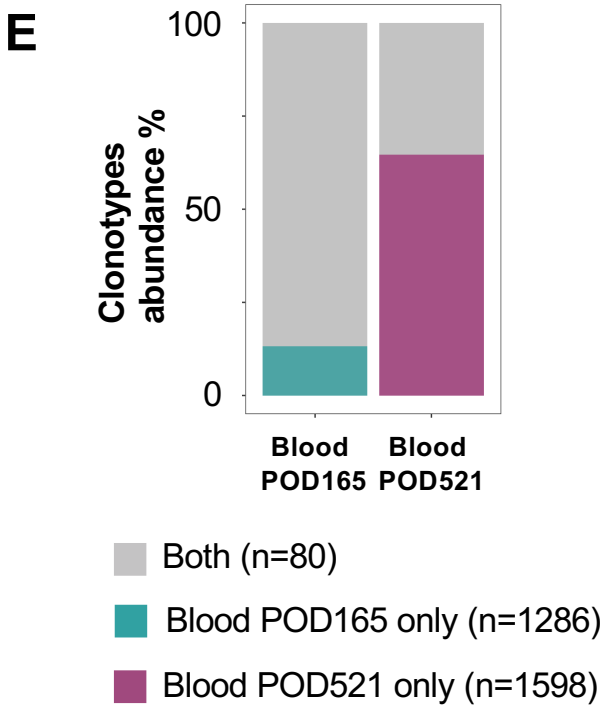
E
Clonotypes abundance %
100
50
0
Blood POD165
Blood POD521
Both (n=80)
Blood POD165 only (n=1286)
Blood POD521 only (n=1598)

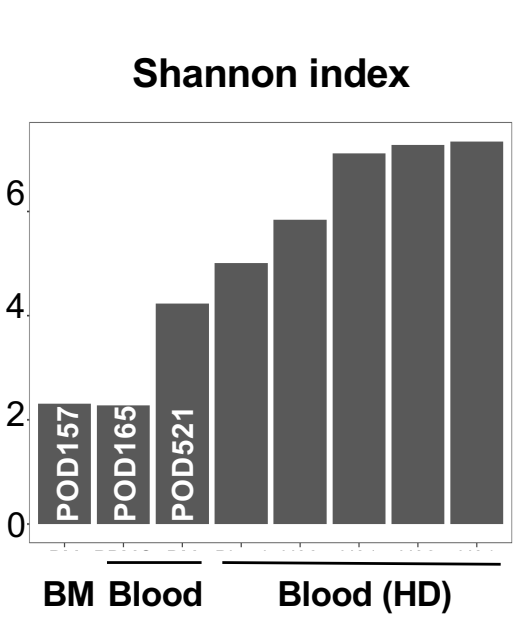
F
Shannon index
POD157
POD165
POD521
BM
Blood
Blood (HD)

Figure S1

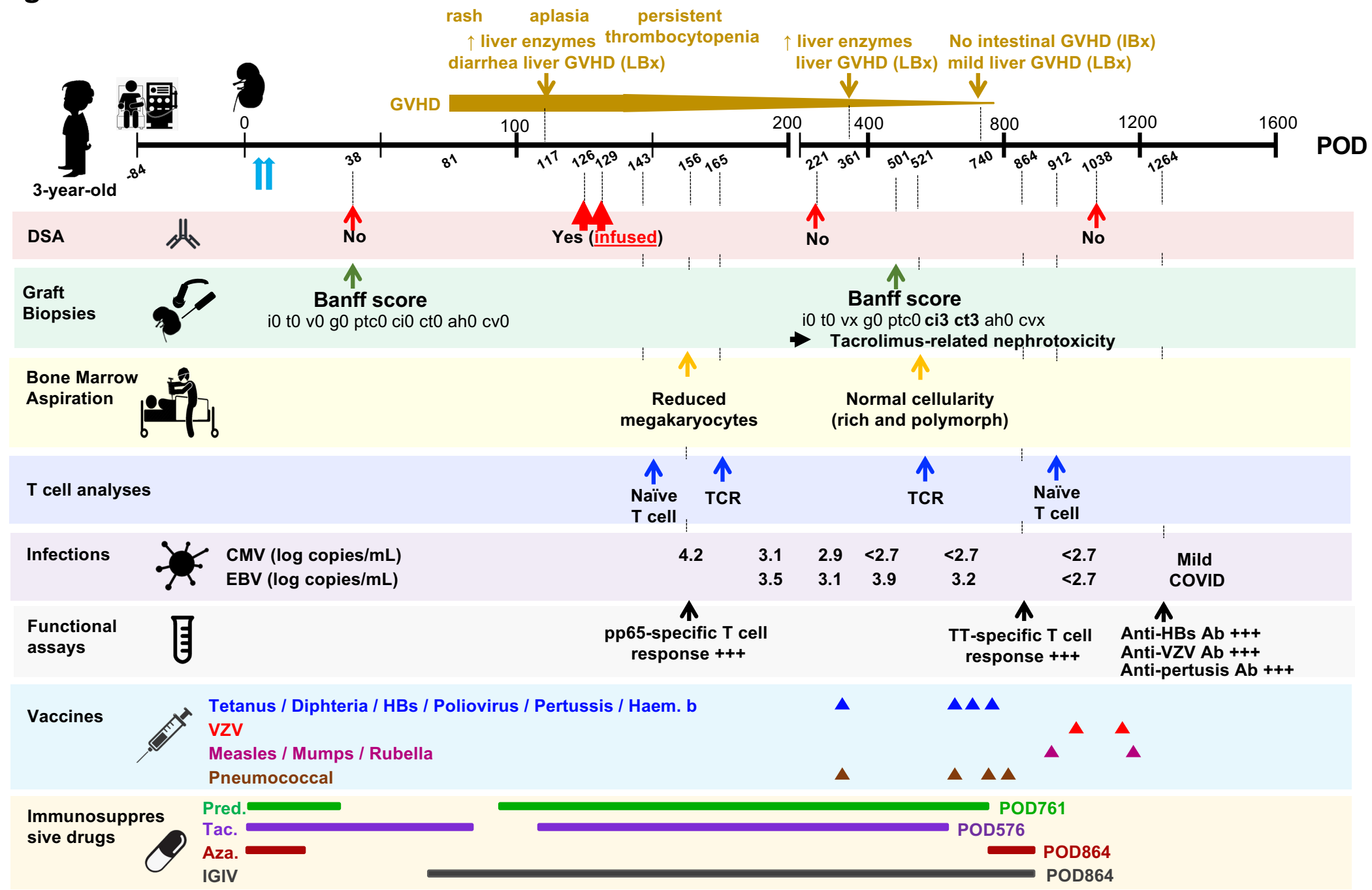
rash
aplasia
persistent thrombocytopenia
↑ liver enzymes
diarrhea liver GVHD (LBx)
↑ liver enzymes
liver GVHD (LBx)
No intestinal GVHD (IBx)
mild liver GVHD (LBx)
GVHD
3-year-old
-84
0
38
81
100
117
126
129
143
156
165
200
221
361
400
501
521
740
800
864
912
1038
1200
1264
1600
POD
DSA
No
Yes (infused)
No
No
Graft Biopsies
Banff score
i0 t0 v0 g0 ptc0 ci0 ct0 ah0 cv0
Banff score
i0 t0 vx g0 ptc0 ci3 ct3 ah0 cvx
Tacrolimus-related nephrotoxicity
Bone Marrow Aspiration
Reduced megakaryocytes
Normal cellularity (rich and polymorph)
T cell analyses
Naïve T cell
TCR
TCR
Naïve T cell
Infections
CMV (log copies/mL)
EBV (log copies/mL)
4.2
3.1
3.5
2.9
3.1
<2.7
3.9
<2.7
3.2
<2.7
<2.7
Mild COVID
Functional assays
pp65-specific T cell response +++
TT-specific T cell response +++
Anti-HBs Ab +++
Anti-VZV Ab +++
Anti-pertusis Ab +++
Vaccines
Tetanus / Diphteria / HBs / Poliovirus / Pertussis / Haem. b
VZV
Measles / Mumps / Rubella
Pneumococcal
Immunosuppressive drugs
Pred.
POD761
Tac.
POD576
Aza.
POD864
IGIV
POD864

Figure S2

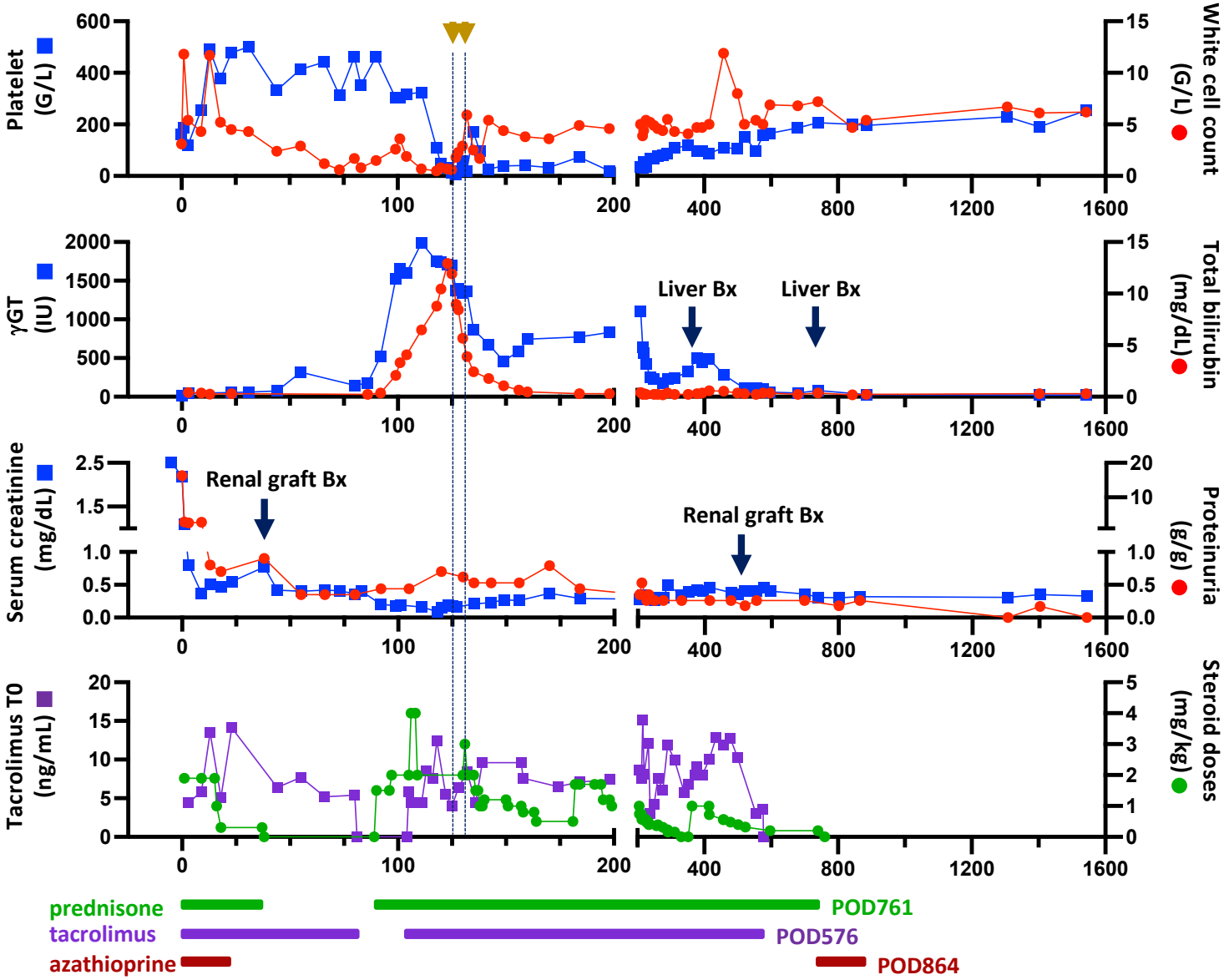
Platelet (G/L)
White cell count (G/L)
γGT (IU)
Total bilirubin (mg/dL)
Liver Bx
Liver Bx
Serum creatinine (mg/dL)
Renal graft Bx
Renal graft Bx
Proteinuria (g/g)
Tacrolimus T0 (ng/mL)
Steroid doses (mg/kg)
prednisone
tacrolimus
azathioprine
POD761
POD576
POD864

Figure S3

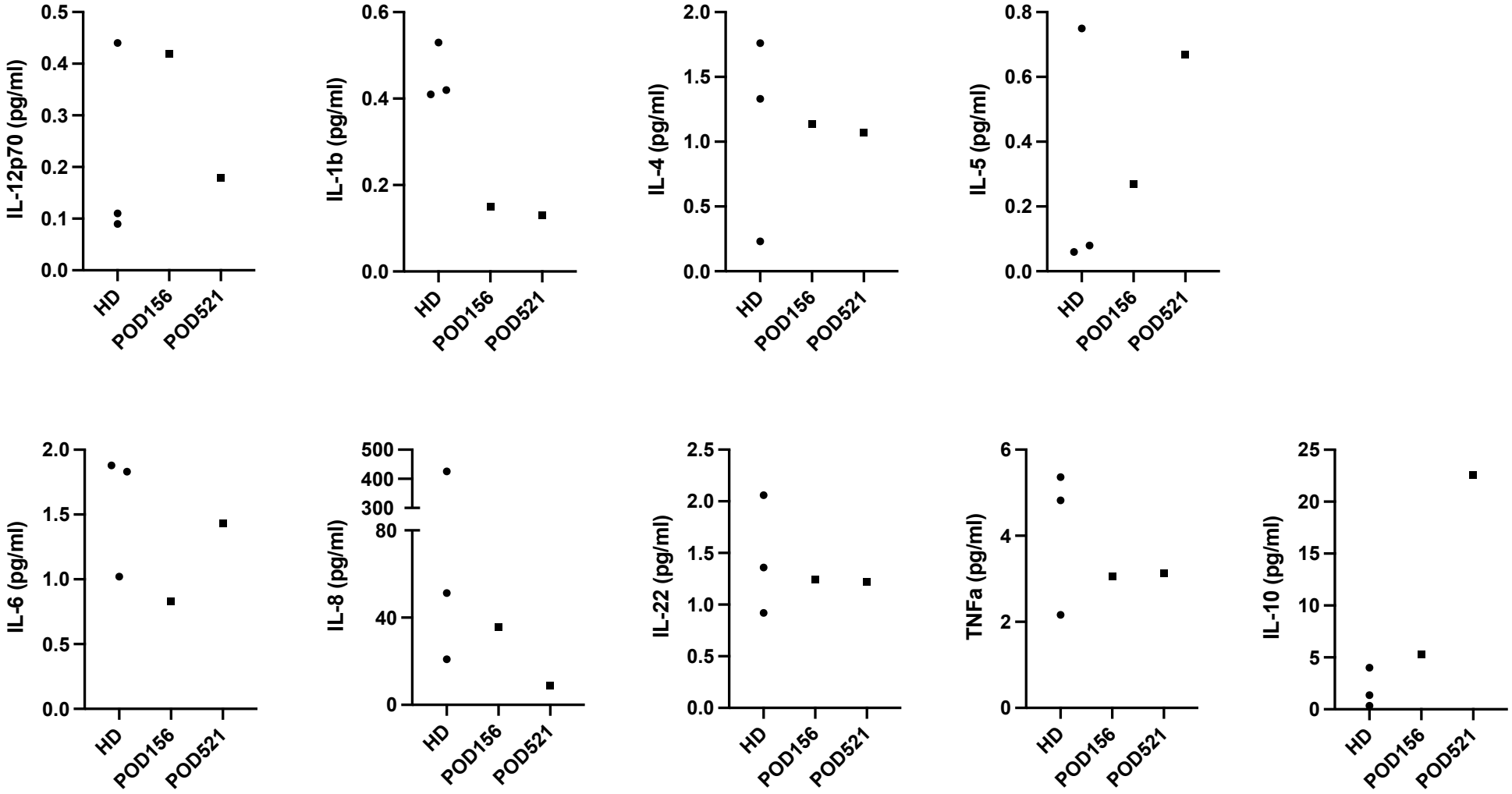
IL-12p70 (pg/ml)
0.5
0.4
0.3
0.2
0.1
0.0
HD
POD156
POD521
IL-1b (pg/ml)
0.6
0.4
0.2
0.0
IL-4 (pg/ml)
2.0
1.5
1.0
0.5
0.0
IL-5 (pg/ml)
0.8
0.6
0.4
0.2
0.0
IL-6 (pg/ml)
2.0
1.5
1.0
0.5
0.0
IL-8 (pg/ml)
500
400
300
80
40
0
IL-22 (pg/ml)
2.5
2.0
1.5
1.0
0.5
0.0
TNFa (pg/ml)
6
4
2
0
IL-10 (pg/ml)
25
20
15
10
5
0

Table S1

HLA loci	A		B		C		DR		DQB		DQA		DP	
D	23	74	65	65	8	8	8	11	5	7	1	5	1	1
R	2	2	18	35	4	7	1	11	5	7	1	5	2	4

Table S2

Immune Features [normal range]	Time relative to kidney transplantation (Days)																
	-92	-66	2	38	58	80	164	184	238	290	311	436	576	698	864	1199	1542
CD3+ [1.4-3.7] (G/L)	0.40		0.15	0.08	0.06	0.06	0.82	0.60	0.32		1.1					3.62	2.89
CD3+ CD4+ [0.7-2.2] (G/L)	0.29		0.12	0.05	0.03	0.03	0.10	0.15	0.07		0.4	0.76	0.85	1.16	1.16	1.79	1.46
CD3+ CD8+ [0.5-1.3] (G/L)	0.07		0.02	0.02	0.02	0.03	0.62	0.38	0.23		0.61	1.19	0.96	1.53	0.84	1.70	1.30
CD45RA+/CD4+ [58-70] (%)	65		52	ND	ND	ND	ND	ND	ND		39					72	62.9
CD45RA+ CD31+ /CD4+ [43-55] (%)	36		41	ND	ND	ND	ND	ND	ND		32					55	49.7
CD45RA+ CCR7+ /CD8+ [52-68] (%)	39		74	ND	ND	ND	ND	ND	3		8					59	54.8
CD16+ CD56+ [0.1-0.7] (G/L)	0.07		0.02	0.02	0.01	0.02	0.12	0.24	0.19		0.27		0.37	0.36		0.22	0.20
CD19+ [0.32-12.4] (G/L)	0.44		0.60	0	0	0	0	0.02	0.02		0.12	0.35	0.09	0.13		0.52	0.62
IgM [0.54-1.53] (g/L)		0.65		0.44	0.23	0.16	0.13	0.14	0.05	0.37	0.44	0.66	0.76	0.48	0.34	0.52	0.85
IgA [0.41-1.41] (g/L)		0.84		0.85	0.59	0.43	0.10	0.13	0.09	0.29	0.31	0.85	0.57	1.34	1.93	2.82	4.36
IgG [5.49-10.19] (g/L)		11.1		6.53	6.60	7.40	8.15	12.2	9.86	9.63	11.75	8.29	10.9	9.88	8.97	7.54	10.91